Universal growth of islands driven by ion beams: Theory and measurements on Pt(111)

C. P. Flynn, W. Swiech, and M. Ondrejcek*
Physics Department and Materials Research Laboratory, University of Illinois, Urbana-Champaign, Urbana, Illinois 61801, USA
(Received 21 March 2008; revised manuscript received 7 July 2008; published 15 August 2008)

We report quantitative measurements of island growth on Pt(111) driven by irradiation with self ions. These processes take place on pans or mesas that isolate the active terrace from the remaining crystal by a surrounding step bunch. The observed evolution takes a universal form common to both growth and shrinkage, dependent on the ion beam energy, for both adatom and advacancy islands. We explore both the functional form and the absolute time scale of the island development. A theory that includes defect reactions is presented to explain the universality, using a quasistatic approximation for the transient defect population. For reasons that are explained, neither the functional form nor the absolute time scale of the evolution depends on the defect diffusion coefficient. Within the uncertainties, the experiments confirm the predicted universal form of the driven island evolution. The quantitative agreement makes studies of island growth an attractive future means for determining the number of surface thermal defects created per incident ion. It also confirms the precision of the molecular dynamics simulations that were employed in earlier research to calibrate the rates at which mobile thermal defects are created during irradiation by self-ion beams of various energies.

DOI: 10.1103/PhysRevB.78.075420 PACS number(s): 68.55.A−, 68.37.Nq, 68.49.−h

I. INTRODUCTION

A beams of self-ions can be used to grow new crystal, as in epitaxial growth from a beam of low-energy ions,[1–3] or to erode a crystal surface by sputtering, using a beam of high-energy ions.[4–6] In effect, the low-energy beam places mobile adatoms onto the surface and, under appropriate conditions, these accrete to form islands from which new crystal planes grow.[7,8] Self-ion impacts of high energy, on the other hand, create excess mobile advacancies, left behind as atoms sputter from the surface into vacuum, and these can accrete to form advacancy islands that grow to erode entire crystal planes.[9–11] In a third process, termed sublimation, advacancies are formed as atoms sublime spontaneously into the vacuum[12] at temperatures sufficiently close to the melting temperature T_m, and processes of accretion and erosion result similar to those during sputtering. Sublimation thus creates a beam of substrate atoms of thermal energy, traveling in the opposite direction, away from the surface. This paper concerns the universality of island evolution among these three processes of sublimation and beam-induced growth and erosion, subsequent to island nucleation, and in the regime of high temperatures in which adatoms and advacancies are mobile.

Both beam-induced growth[1–3,7,8] and beam-induced erosion[4–6,9–11] have been widely studied, and the microscopic evolution of surfaces during sublimation[12,13] has been a topic of recent interest for elemental semiconductors[14,15] and clean metal surfaces.[16,17] Each of the phenomena attract both scientific and technical interest[8,10] particularly the pattern formation that decorates the surfaces as it evolves in the different cases.[11] Sublimation is, of course, generally confined to the highest temperatures, but growth and erosion may occur at both high and low temperatures. It was recognized in early publications[18,19] that the consequences of the Gibbs-Thompson effect, by which the stiffness modifies the chemical potential, differs in the two temperature ranges, and that the critical radius for nucleation becomes small at low temperature, where much research focuses.[1,7]

Several papers report that island radii grow almost linearly with time (with possible sublinear corrections), at least in the later stages of growth at high temperatures. Examples of representative data for metals and semiconductors that support this viewpoint are referenced and reproduced in Fig. 1. There remains a need for investigations that cover evolution over the entire range of island size, and for detailed comparisons among the behaviors observed in the three separate processes.

This paper reports efforts to document the evolution of island growth under the driving force of a steady self-ion beam of fixed energy. We are concerned with both the functional form of the time variation and its absolute time scale. The observations were made possible by a low-energy electron microscope (LEEM),[20] in whose images the step edges

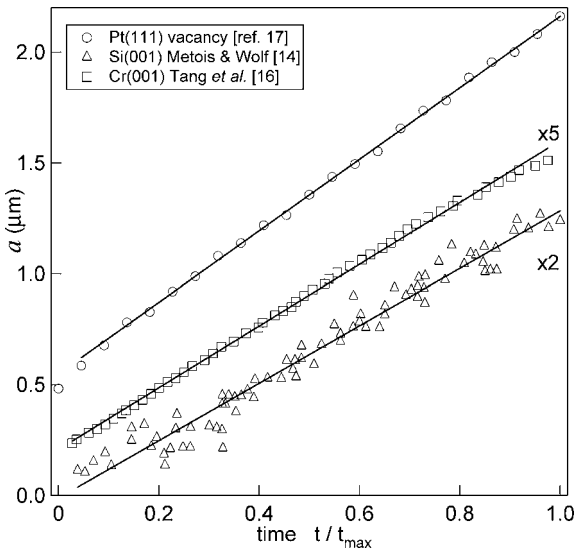

FIG. 1. Growth of advacancy island radius a with time t is approximately linear for reported cases of sublimation at 1410 K (triangles) on Si(001) (Ref. 14), on Cr(001) (Ref. 16) at 1186 K (square points), and growth on Pt(111) at 1125 K (Ref. 17) (circles).

 ©2008 The American Physical Society

that form the perimeters of islands can be made visible by interference contrast. The instrument was fitted with an ion accelerator that offered tunable ion energy such that surface processes driven by a selected beam could be followed over a wide range of conditions.[21] Given both adatom (low-energy) and advacancy (high-energy) beams, and both adatom and advacancy islands, it is possible to examine the driven growth and shrinkage for islands of both signs. Observations of the resulting behavior are presented in Sec. II D below. A theoretical discussion in Sec. III, following earlier results,[22] predicts universality in driven growth, and is compared to the experimental results in Sec. IV. Sufficient details of the equipment to make the experiments comprehensible are included below in Sec. II A, and Secs. II B and II C, respectively, discuss sample handling and experimental procedures. The manner in which a beam of self-ions initially causes islands to nucleate is a separate topic, described in some detail elsewhere.[23]

Driven island growth includes diffusion behavior in which surface defects are transported across the sample surface.[2,7,8] Without doubt, the transport is sensitive to boundary conditions established by the sinks at which these point defects equilibrate,[22] typically surface steps.[2,7] It is apparent that similarities of behavior among diverse processes can be then established only to the degree that the perturbations caused by redundant surface structures, such as free step edges, strains, or blemishes, can be made negligible. In the present work, an effort has been made to control such extraneous influence by confining the growth studies to islands near the centers of roughly circular pans or mesas. Mesas are formed when a single terrace is surrounded by a bunch of outward-directed steps that isolate it above the level of the remaining lattice. Pans are similar, but with inward-pointing steps, that isolate the terrace below the level of the nearby surface. In recent work[22] we show how pans and mesas can be created by means of ion beam processing from typical clean metal crystal surfaces. Here we examine island growth on pans and mesas that decouple the island evolution from defect sinks located outside the step bunches that contain these structures. The theory of driven island growth, presented in Sec. III and Appendix, is adapted to this chosen geometry.

The system selected for study is clean Pt(111) bombarded by Pt^- ions. This is a surface well adapted to the requirements of surface cleanliness required by the experiments. It also offers the advantages of earlier detailed measurements of surface diffusion on Pt(111) both by step fluctuation spectroscopy[25] and by the decay of Fourier step profiles synthesized using ion beams.[26] The former investigations determine, in addition, the temperature- and orientation-dependent step stiffness on Pt(111). A known complication is the fact that the life cycles of adatoms and advacancies under the present conditions are dominated by pair processes of spontaneous creation and recombination on perfect terraces,[25,27] rather than by independent processes for the two species at fixed sinks. A theoretical description of transport over the surface is accordingly modified. The theory of universal evolution in driven growth, outlined in Sec. III and Appendix, accommodates the need to describe transport in a reacting defect assembly.

II. EQUIPMENT AND EXPERIMENTAL RESULTS

A. Equipment

In the research reported below, the surfaces under examination were observed using a LEEM designed and built by Tromp[20] at IBM Corp., Yorktown Heights, NY. The important features for the present work is that the LEEM maintained a vacuum of 10^{-10} torr while operating on a Pt(111) sample at temperatures up to 1400 K, and produces images with about 10-nm resolution of atomic step edge structures. The LEEM was fitted post manufacture with a SNICS II negative ion accelerator, built by National Electrostatics Corp, that provided an intense beam of Pt^- ions on the sample. The accelerator operated by Cs^+ ion sputtering of a Pt metal target. It provided Pt^- ion impact rates on the crystal up to ~ 0.2 ML/s over a circular target area 1 mm in diameter, collimated to the sample center by a liquid nitrogen-cooled beam dump located axially inside the objective lens. Fluxes of this magnitude were available with mean impact energies tunable from 0 to 5 keV, with 50 eV half width of energy spread, while the system remained within the vacuum constraint stated above. It was possible to image the surface during actual irradiation. Some complication of imaging condition was apparent at the highest ion fluxes, owing to space charge effects arising from the coincidence of paths between the electron beam used for imaging and an intense ion beam operating close to its space charge limit.

A full description of the tandem machine is available elsewhere.[21]

B. Materials

The Pt single crystal used in this work was purchased from the Surface Preparation Laboratory, The Netherlands. It was 9 mm in diameter and 0.9 mm thick, cut within 0.2° of the (111) plane. The required surface cleanliness was achieved[25] by cycles of 1-keV Ar^+ ion bombardment, followed by annealing at 1300 K, with occasional treatment in 10^{-6} Pa O_2, first in an external chamber and later in the LEEM vacuum. These methods are detailed elsewhere.[25] The eventual surface exhibited sharp (1×1) LEED reflections with no trace of impurities detected by LEED or Auger probe with 1% sensitivity. The Pt target used by the SNICS II source was 99.99% Pt with principal impurities of other noble metals. It is a characteristic of the source that the exiting beam contains a fraction $\sim 10^{-4}$ of Cs atoms. In our equipment these were removed from the beam by deflection into a beam dump cooled to liquid nitrogen temperature.

No sign of Pt(111) surface contamination attributable to the ion beam was observed in our experiments.

C. Experimental procedures

It will be shown in Sec. III and Appendix that the evolution of islands is sensitive to the geometry of the surrounding sinks that drain off part of the excess thermal defects created by the ion beam. For this reason it is important that mesas or pans can be created to isolate the island kinetics within a reproducible step bunch boundary.

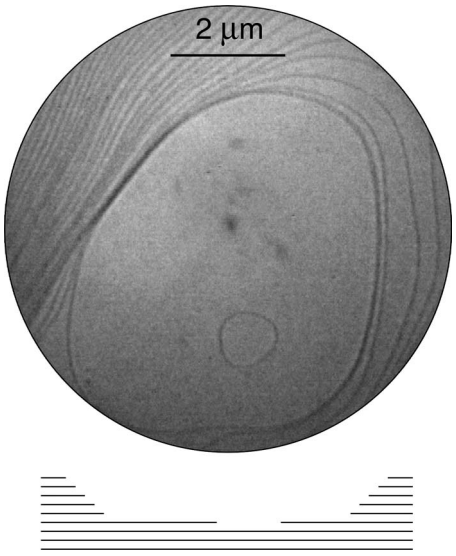

FIG. 2. LEEM image of pan with maximum dimension ~6 μm, created on Pt(111) by irradiation with 515 eV Pt^- ion beam (see text) using 6.9 μA cm^{-2} at 1140 K. A vacancy island nucleated by an increase in ion beam intensity is seen on the pan terrace. Atomic planes that form the structure shown are indicated schematically below the image. The LEEM impact energy is 17 eV.

A pan comprises an atomically flat surface terrace contained by a high peripheral bunch of steps that step-up with increasing radius; a mesa is the same but with a step bunch that steps down.[24] A LEEM micrograph of a pan is shown as an example in Fig. 2, with a cartoon of the profile below. The pan is shown with a freshly nucleated vacancy island near its center, also present in the cartoon. It is reported elsewhere how, with the aid of the SNICS II ion beam, it is possible to create mesas and pans from local maxima and minima on an initially clean, almost flat surface. The trick is simply to adjust the irradiation parameters over time in order to inhibit the nucleation of new islands. The behavior is detailed and explained elsewhere.[24]

Once the structure is formed, it is a simple matter to nucleate either new adatom or advacancy islands as shown, by means of an increase in intensity of a beam of suitable energy. New islands generally form near, but not exactly at, the center of the structure, as shown in Fig. 2, for reasons that are understood.[22] Off-center islands shift as they grow. There is sufficient scatter of location that the two factors of position and shift generally limit the radius up to which growth can be sensibly universal. Upon exposure to a continued beam, adatom islands grow when driven by a beam with energy less than a "neutral" value ε (i.e., an "adatom beam," yielding hyperthermal epitaxial growth), and shrink under a beam with energy greater than ε (an "advacancy beam" that causes erosion). For Pt(111), $\varepsilon \approx 250$ eV.[17]

The driven growth of an adatom island on a mesa causes only slight enlargement of the mesa because of the small ratio of net defect precipitation between the island and the peripheral step bunch, given that the step bunch accommodates fresh adatoms on a large number of levels.[24] Similar comments hold for the growth of advacancy islands on pans.

In the two converse cases (e.g., adatom island on a pan) the adatom beam causes the island to grow but causes an inward motion of the step bunch. Specifically, it detaches the innermost step from the bunch and causes its radius to decrease progressively with time.[24] Consequently there is a limited experimental period available to observe a central adatom island grow under an adatom beam before the encroaching step materially alters the effective geometry of the perimeter. This characteristic makes the two converse cases somewhat more difficult to investigate.

It will be evident that a sufficient mobility of the thermal defects created by the beam is required for island growth to occur. The ability to purposefully create isolated individual islands using the beam is itself a criterion that the mobility is sufficient since roughening (spontaneous formation of many small islands) is thus absent. The perspective from which these effects are viewed in Sec. III is that the thermal defect population, created by the beam, establishes position-dependent defect concentrations on the terrace. The flow of defects down the gradients then follows from the surface mass diffusion coefficients D of adatoms and advacancies. In earlier independent studies, the net surface mass diffusion coefficient D_s has been determined[25,26] for Pt(111) over a large variation of a factor $\sim 10^6$ between 710 and 1520 K and processes at steps determined to be diffusion-(rather than reaction-) limited. The present investigations were carried out within this range, where the defect mobility is sufficient. We show later, however, that the rate at which islands evolve is independent of the surface diffusion coefficient. The explanation for this curious fact is that the defect distribution builds up to a steady state in which defect creation is exactly balanced by the flow of excess defects to sinks. Controlled observations of island growth within these constraints are reported in what follows.

D. Experimental results

Figure 3(a) identifies two orthogonal lines AB and CD drawn through a diameter of an adatom island on a mesa of dimension ~6 μm. This typical island, used here for the purpose of illustration, exhibits the threefold symmetry expected of the (111) plane of fcc Pt metal. The anisotropy is nevertheless small and will be neglected in this discussion. In particular, the intersections of the chosen diameters with the island step are employed here as measures of the island radius, $a(t)$, during growth.

In the experiments reported below, two alternative procedures were followed. For islands and arenas (i.e., pans or mesas) of the same sign, the beam intensity was gradually increased in small steps until the central island nucleated. Growth could thus be followed, if desired, from the instant of nucleation ($a=0$, within the available resolution) through the entire growth until the island merged into the peripheral step bunch. From the video record of one such sequence we have extracted the pixels of the particular rows represented by the chosen diameters. In Fig. 3(b) these are presented with vertical displacements, to form a single figure. The resulting images, successively displaced in Fig. 3(b), provides a visual record of the island radius, marked by the contrast change caused by the step, as a function of time, t, from the nucleation event ($t=0$) onwards. White bands are blanks during

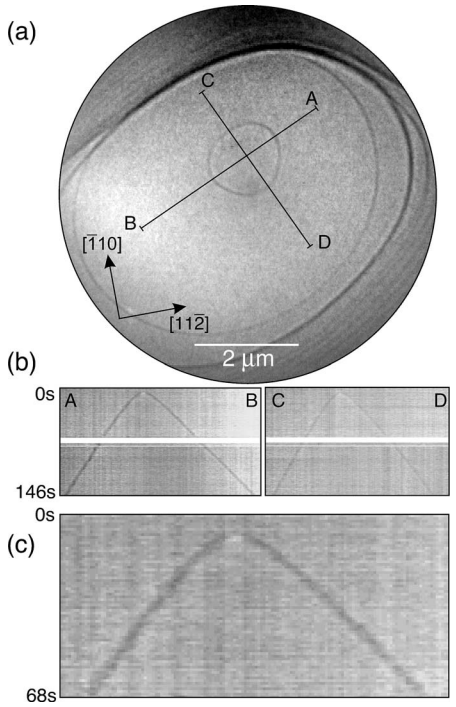

FIG. 3. (a) Two diameters AB and CD of an adatom island on a mesa are shown, as employed here to determine a "radius" $a(t)$ of the evolving island. Note that the actual island shape has threefold symmetry characteristic of Pt(111). (b) Image rows along the diameters extracted from successive images and displaced vertically. These provide clear traces of island evolution with time following nucleation, at 1130 K, by 65 eV Pt^- ions, at flux density 5.5 μA cm^{-2}. Blank intervals occur where the microscope was adjusted. (c) Expanded view of growth near $t=0$ immediately after nucleation. The almost linear growth observed at larger radii in (b) does not extend through the early regime.

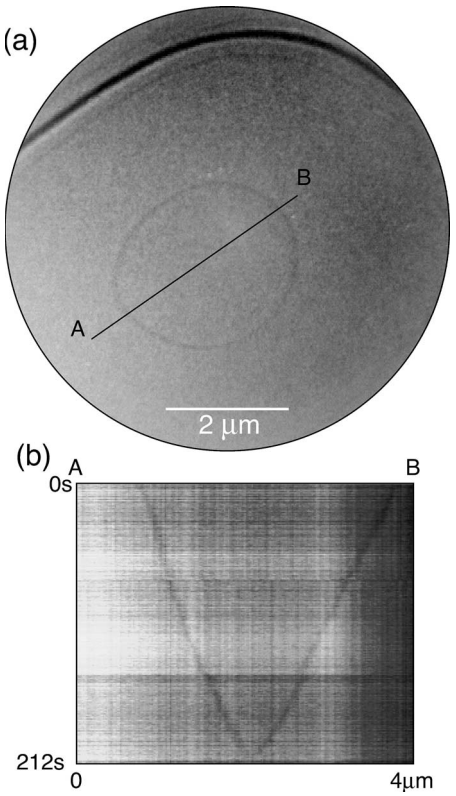

FIG. 4. (a) Adatom island with $a \sim 0.5$ μm, grown on a mesa. (b) Evolution of island diameter at 1130 K during shrinkage caused by a 515-eV advacancy beam (i.e., energy greater than neutral energy). Note, as in Fig. 3, that the evolution is no longer linear in time as the island vanishes. Flux density 5.5 μA cm^{-2}.

routine machine adjustments. Realignments, using defect or step bunch images as reference points, were occasionally needed to compensate for image drift. In the case shown, the island nucleated somewhat off-center of the area, and the trace of the two radii departs from exact symmetry as a consequence. After an initial period, the radius is seen to change with time almost linearly, just as in earlier reports of sublimation and of driven growth cited above. Near $t=0$, however, the evolution in Fig. 3(b) departs markedly from the linear trend. This is revealed more clearly in Fig. 3(c), which presents an enlarged view of the behavior along diameter AB shortly after nucleation. The growth of $a(t)$ near $t=0$ appears more parabolic than linear. This is in evident contradiction with theories that predict a linear variation.[16]

In the second of the alternative procedures, an island was created, say for example an adatom island, under the influence of an adatom beam, as in Fig. 4(a). At a selected size, the beam energy was increased, changing the irradiation to an advacancy beam. The island then shrank and its shape was followed until it vanished at radius zero. Once more the video record could be employed to create a trace of the time sequence of island radii. Figure 4(b) gives an example of the observed evolution close to $a=0$. The trace there is again more parabolic than linear.

An important observation connects the two cases of driven growth and driven shrinkage of islands. Figure 5 includes the growth of adatom islands as crosses and the shrinkage of adatom islands as open circles. The ordinate is $x=a/R$ with R the average radius of the (generally noncircular) terrace on which the process occurs. The time is reversed for shrinking, with the time axis scaled to make the evolutions as similar as possible. This comparison is very successful, with the two time evolutions both approximating a single path. The scaling factors required to attain the most similar evolutions were recorded for use in a subsequent discussion of absolute rates. The features noted in these illustrative examples are characteristic of all data taken in the present investigations of driven island processes, for both adatom and advacancy species. A global comparison of both the functional forms and the absolute rates is presented in Sec. IV below.

While satisfactory when a is small relative to R, the present experiments lose precision for large islands, as $a \rightarrow R$. The experimental problem is that islands rarely nucleate at the exact center of a terrace. Moreover, the islands observed in our research are almost circular, augmented by a weak threefold character that is derived from anisotropy of the step energy on Pt(111) at these temperatures. This symmetry contrasts with the terrace shape, which retains complications from the specific surface topology from which the pan or mesa was initially created. As the island step and the

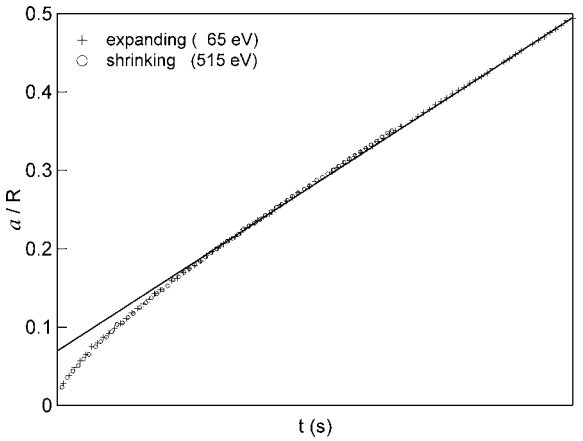

FIG. 5. Growth and shrinkage of adatom island shown superposed. Time is shown reversed for shrinkage. The ion beams employed had energies of 65 eV (growth using adatom beam) and 515 eV (shrinkage using advacancy beam). With the times scaled to match, the two evolutions follow closely similar paths in reverse directions. The time interval for the growing island is 0–90 s, for the shrinking island 0–380 s.

terrace perimeter have generally differing shapes, a growing island must necessarily make contact with the perimeter step bunch at different times that depend on the angular position of the contact point around the circuit defined by the step bunch. For this reason, the above data plots that show growth of the scaled radius $a/\bar{R}$ employ an effective (rms) radius $\bar{R}$ that is averaged over angles.

III. THEORY OF ISLAND EVOLUTION

The observation that the evolution takes a similar form for growth and shrinkage of islands suggests that the driving mechanisms are identical as a function of island geometry, fixed by the radius, a. The discussion given here presumes that the precipitation process is known[25] to be diffusion limited (rather than influenced by defect reaction times at steps), for reasons clarified below. A reasonable inference is that the diffusion field is quasistatic, since it is evidently not greatly affected by the growth velocity (which changes sign between growth and shrinkage) with which the island radius is changing. Quasistatic here means that the rates at which the radius and concentrations change give a negligible contribution to the fluxes, which thus arise predominantly from existing gradients. A cartoon in Fig. 6(a), limited to radii $r \ll R$, suggests how concentration gradients near islands are generally increased by growth (arrow pointing right) and decreased by island shrinkage (arrow pointing left). Also, in the Gibbs-Thompson effect, the step curvature changes the chemical potential at the step by $\delta\mu^*$, and causes adatoms to evaporate onto the terraces from adatom islands, and advacancies from advacancy islands. This process evidently favors island shrinkage. It is indicated in Fig. 6(b) how the added chemical potential at the step changes the gradients that drive evolution. Broken lines indicate chemical potentials for an advacancy beam (lower) and adatom beam (upper) with $\delta\mu^*=0$. With $\delta\mu^*$, the gradient for an advacancy beam (solid line, with left pointing arrow showing vacancy flow) is now larger than that for an adatom beam (right pointing arrow and solid line). From the similarity of observed growth and shrinkage rates we infer also that the Gibbs-Thompson effect plays a negligible role under the conditions of the experiments. Indeed, this is confirmed, first by the observation that island radii remain fixed in the absence of a beam, and second by calculations using known step stiffness to estimate the flux driven by the Gibbs-Thompson potential, which proves to be negligible under the present conditions.

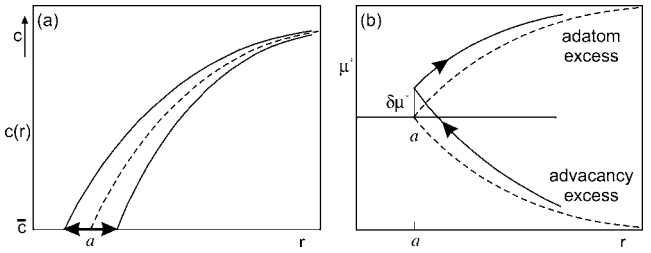

FIG. 6. Sketches showing gradients of concentration (a) and chemical potential (b) for $r \ll R$, near an island step, in order to clarify two effects on growth: (a) Arrow directions show radius changes in growth (right) and shrinkage (left); solid lines indicate the resulting defect concentration profiles. Growth increases the gradient and so increases the rate, whereas shrinkage decreases the gradient and slows the rate. (b) The Gibbs-Thompson effect changes the chemical potential at an island by $\delta\mu^*$, with opposite effects on the gradients driving growth by an adatom beam (upper solid line) and an advacancy beam (lower solid line). The arrows represent the directions of advacancy flow in the two cases. The processes shown in (a) and (b) both tend to break universality.

By this reasoning we are thus drawn to a description of the process in which the diffusion field is quasistatic, with all evolution stemming from the spatial distribution of defect concentrations thus defined, and neglecting defect evaporation from the island.

On the basis of a recently published theory,[22] it is shown in Appendix that the flux of atoms over the surface at $\mathbf{r}$, driven by creation rates K_1 and K_2 per surface site per second of adatoms and advacancies, respectively, is

$$J(\mathbf{r}) = -D_1 \nabla s_1 + D_2 \nabla s_2 = (K_1 - K_2) \nabla f(\mathbf{r}).$$

[see Eq. (A3)]. Here, $f(\mathbf{r})$ is the solution of the Poisson equation $\nabla^2 f = 1$ with the boundary condition $f=0$ for the step edge sinks at $r=a$ and $r=R$. These boundary conditions are appropriate when defect reactions at steps are fast enough that they play a negligible role in limiting the kinetics. This is known to be the case from the wavelength dependence of relaxation observed for Pt(111) by step fluctuation spectroscopy.[25] In the present case the solution inside the island (i.e., for $r<a$) is

$$f_<(r) = (r^2 - a^2)/4,$$

[see Eq. (A4a)]. For $a<r<R$ on the terrace outside the island, the solution is

$$f_>(r) = \frac{r^2 - R^2}{4} - \frac{(a^2 - R^2)\ln(r/R)}{4\ln(a/R)}.$$

[see Eq. (A4b)].

In the flux density given by Eq. (A3), the gradient term from $r<a$, using Eq. (A4a) cancels the first term on the right of Eq. (A4b) for $r>a$, to leave the entire flux density determined by the Laplacian term

$$\nabla[f_< + f_>]_{r=a} = \frac{R^2 - a^2}{4a\ln(a/R)}. \quad (1)$$

The rate of step advance for an adatom island with an adatom beam is now obtained from the area A added per precipitated adatom as

$$da/dt = J(a)A \quad (2)$$

or from Eqs. (A3) and (1),

$$\frac{dx}{d\tau} = \frac{(x^2 - 1)}{x\ln x};$$

$$x = a/R; \quad \tau = (\Delta K/4)t, \quad (3a)$$

in which $\Delta K = K_1 - K_2$. A second form of this result is

$$\frac{dS}{d\tau'} = \frac{S - 1}{\ln S};$$

$$S = x^2 = (a/R)^2; \quad \tau' = \Delta K t. \quad (3b)$$

Equations (3a) and (3b) have solutions related to the logarithmic integral $\mathrm{li}(x)$ and cannot be written in a finite number of terms. Power series solutions for the (scaled) time τ required to attain an island size x, S, are as follows:

$$\tau = -4x^2\left[\ln x\sum_{p=0}^{\infty}\frac{x^{2p}}{2(p+1)} - \sum_{p=0}^{\infty}\frac{1}{4(p+1)^2}\right], \quad (4a)$$

$$\tau' = -S\left[\ln S\sum_{p=0}^{\infty}\frac{S^p}{p+1} - \sum_{p=0}^{\infty}\frac{S^p}{(p+1)^2}\right]. \quad (4b)$$

The forms of these two solutions are shown in Fig. 7 for the relevant domain $0<x, S<1$. It is notable that the behavior of $x(\tau)$ near $\tau=0$ clearly resembles the island evolution documented above in Sec. II D. We return to this topic below.

It is a remarkable result that neither the pathway nor the absolute rate of the island evolution predicted by Eqs. (3a) and (3b) depends on the diffusion coefficients of the mobile thermal defects that transport the surface atoms involved in the growth. The result is purely geometrical, but does depend on diffusion-limited flow. This remains true provided that the mobility is large enough to avoid roughening, and is constant throughout the process. The explanation is that the defect concentrations built up by irradiation rise to levels inversely proportional to the diffusion coefficient, which thus cancels from the flux $\sim D\Delta c$. In the steady state, the net flux to sinks exactly equals the net creation rate of defects, independent of diffusion rates.

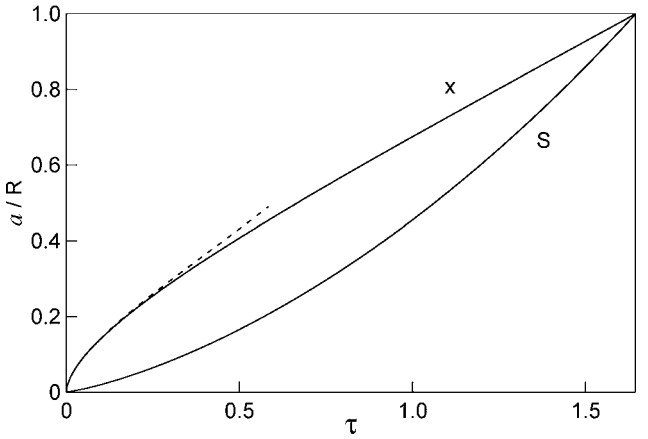

FIG. 7. Scaled island radius $x=a/R$ and scaled island area $S=a^2/R^2$ both shown as functions of scaled time $\tau=(\Delta K/4)t$ using the expansion in Eq. (4a). The first term of $x(\tau)$, $x^2\ln x$, is indicated by a broken line to show how it correctly approximates the behavior near $\tau=0$.

The leading terms of the expansions in Eqs. (4a) and (4b) are not analytical near $\tau=0$, in keeping with the way the differential equations [Eqs. (3a) and (3b)] behave there. In Fig. 7, the magnitude of the leading term, $\tau\sim 2x^2\ln x$, is indicated by a broken line to show that near $\tau=0$ it faithfully predicts the full result. Thus the rounded evolution for small radii observed in the experiment originates directly from this nonanalytical term.

IV. UNIVERSALITY

It is clear from Eqs. (3a), (3b), (4a), and (4b) that the predicted growth behavior is entirely universal for the case treated, in which a circular island grows or shrinks at the center of a circular terrace. S is the island area, scaled by the terrace area, and τ, τ' are times rendered dimensionless in Eqs. (3a) and (3b) by factors related to the rate of net defect creation ΔK. No parameters other than S (or $x=\sqrt{S}$) and τ, τ' determine the island evolution for this universal form. Note that for the growth of advacancy islands, a minus sign must be inserted on the right of Eq. (2) because the adatom flux causes shrinkage (da/dt negative); but as ΔK must also now be negative in Eqs. (3a) and (3b), the growth equations remain unchanged. In the converse cases where the combination of island sign and beam sign result in shrinkage, a single minus sign enters the growth equations and the sign of the derivative they describe is reversed. Then the system travels the same universal growth trajectory but in the opposite direction, as the radius decreases with time. This is the case for adatom islands in an advacancy beam and for advacancy islands in an adatom beam. We note in connection with Eqs. (3a) and (3b) that the growing island captures a larger share of the defects created by the beam than its area alone explains, relative to the terrace area. Specifically, at radius a, the island absorbs a fraction

$$f(a) = \frac{S - 1}{\ln S} \quad (5)$$

of the entire defects created on the pan or mesa, of which only a fraction S are created directly inside the island. As a

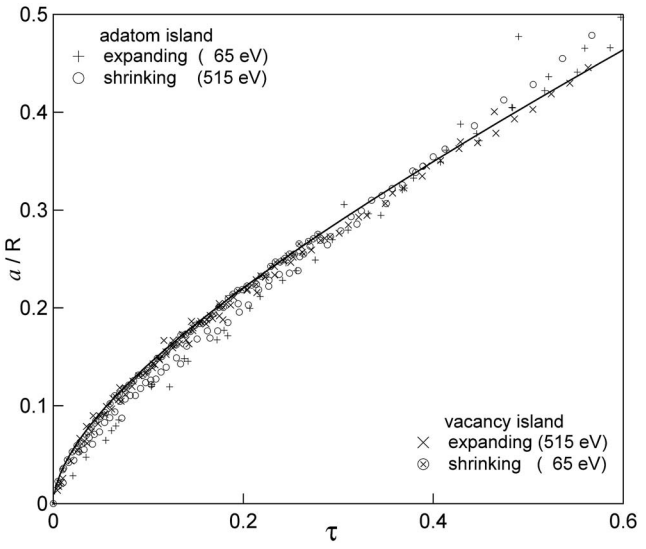

FIG. 8. Universality of data for scaled growth and shrinkage at early times, shown by the superposition of scaled data from 10 cases, including adatom and advacancy islands, and both growth and shrinkage. The times are scaled to make the data coincide with the predicted functional form of the evolution (see text).

$\rightarrow R$ we find, by writing $a=R(1-\delta)$, that the fraction becomes approximately

$$f(a) \rightarrow \frac{1}{1+\delta^2/3}, \quad \delta=(R-a)/R \rightarrow 0. \tag{6}$$

When, in the opposite limit, the island is small, $S \ll 1$ and

$$f(a) \sim 1/\ln S, \quad a \rightarrow 0. \tag{7}$$

This enhancement of island growth arises from defects that are created outside the island and precipitate on the island by diffusion. We find that the multiplier by which the number actually created within the island is increased as

$$-\frac{R^2-a^2}{2a^2\ln(a/R)} = \frac{S-1}{S\ln S}. \tag{8}$$

This ratio diverges as $a \rightarrow 0$. Evidently for the diffusion field on a terrace, it is a poor approximation to assume that those mobile species that precipitate on the island during driven growth originate mainly from processes that take place within the step edge that surrounds the island. Instead, for islands that are small compared to the terrace, the preponderance of the defects that attach to the island diffuse there from initial locations outside the island.

The final topic for discussion here is the extent to which the theoretical evolution, Eqs. (4a) and (4b), of island radius under driven growth, agrees with the experimentally observed processes reported in Sec. II D. There are two parts to this comparison, as will now be explained. The first concerns the functional form of the scaled evolution, for which an initial comparison is provided in Sec. II D. A global perspective is offered in Fig. 8, where data from numerous runs include both adatom and advacancy islands with both growth and shrinkage for each case. Each set of data is scaled in time to best conform to the predicted evolution, which is indicated by the solid line. The required scaling factors λ are compared later to factors predicted directly from beam calibration and the beam currents employed. It is clear in Fig. 8 that the scaled data follow a common trend with good accuracy. The results for longer time lines exhibit the linear trend noted above and depart to a more rounded evolution at short times.

There appears no doubt that the theory provides a reasonable description of the observed behavior at those early times for which universality remains possible because the effect of detailed boundary conditions at the perimeter step bunch is relatively weak. The experimental results do follow a more linear trend than that predicted when the island grows to $a/R \sim 0.5$. The linear results resemble earlier reports of advacancy islands driven by sublimation (see, e.g., Fig. 1). We interpret the deviations as arising from experimental departures from the ideal geometry because the actual island and terrace perimeters are neither exactly circular nor exactly concentric.

The second point for discussion in this connection is the recognition that both experiment and theory determine absolute rates of evolution. The question then arises as to whether or not these two rates are in quantitative agreement. In this regard it is a significant point that an island radius relative to a terrace radius, specifically a/R, is a ratio accurately determined from the microscope images independent of the microscope magnification. For each video sequence, i, the evolution of this ratio was scaled to the predicted form in Fig. 7 by multiplying actual time by a chosen factor λ_i. On the other hand, Eq. (3a) is an exact prediction for the model described in Appendix,[22] given values of the beam calibration ΔK_i and the actual current density for the ion beam used for the particular irradiation, i. In earlier investigations[17] we have obtained absolute values of ΔK per incident ion for all energies by comparing the energy dependence of our observed creation rate of thermal defects with the mass yield values predicted by careful simulations using molecular dynamics (MD).[17,28] For the specific beams employed here the values are $\Delta K=K_1-K_2=0.82$ at $E=65$ eV and $\Delta K=-1.04$ at $E=515$ eV. From these calibration results, upon multiplying by the ion current employed in each present experiment, i, we obtain a second scaling factor λ_i' that is predicted by theory to bring the different observations i onto a common time scale τ. Provided that both the MD simulations and the above theory of the surface processes are accurate, then the values of λ_i and λ_i' should be identical for all i.

To investigate the degree to which the experiments confirm the calculations we have therefore determined λ_i/λ_i' for the experiments reported in Fig. 7. Neglecting one value that deviated from the remainder by a factor three for undetermined reasons, the remaining ratios average to

$$\langle \lambda_i/\lambda_i' \rangle = 1.0 \pm 0.2$$

in place of the expected value of unity. This has a satisfactory degree of agreement among measurements widely spaced in time. The absolute rates of island evolution are thus predicted to a degree comparable with the universality of the functional form.

V. SUMMARY AND CONCLUSIONS

In this paper we report the evolution of adatom and advacancy islands driven by beams of Pt ions on clean Pt(111). For islands less than half the terrace size, the observed growth or shrinkage closely follows a universal form. This form is predicted accurately in functional form and absolute time scale by a theory with a quasistatic approximation to the beam-induced distribution of mobile adatoms and advacancies, and neglects Gibbs-Thompson evaporation of thermal defects from the islands.

Elements in this comparison are results, from molecular dynamics, of the surface defect populations created by self-ion beams of various energies. Our results suggest that for Pt(111) these methods have predictive accuracy, since they contribute as proportionality factors in an accurate prediction of the absolute rates of island growth. From the reverse perspective, it appears from the present results that measurements of island evolution alone may provide an accurate calibration for the rates $\Delta K = K_1 - K_2$ at which an ion beam creates excess point defects. This is a significant opportunity that deserves attention in future research.

Because the functional form of the island evolution is predicted correctly, it is established by the present results that as the island radius decreases, an increasing fraction of the growth takes place by defects that originate from beam-induced creation on the terrace external to the island. There is no evidence that the nucleation process that precedes the quasistatic growth regime has any material effect on island evolution in the later processes investigated here.

ACKNOWLEDGMENTS

This research was supported in part by DOE under Grant No. DEFG02-02-ER46011. The LEEM was maintained in the Center for Microanalysis of Materials in the Materials Research Laboratory, supported by DOE Grant No. DEFG02-91-ER45439.

APPENDIX: DEFECT FLUXES IN A DRIVEN ASSEMBLY OF REACTING THERMAL POINT DEFECTS

Here the goal is to predict the time evolution of island size on a terrace that has its thermal defect population driven by a uniform flux density J of ions. Suppose that the beam creates adatoms at a rate K_1 per surface site per second, and advacancies at a rate K_2, such that the equilibrium concentrations $\bar{c}_1, \bar{c}_2$, per site, of adatoms and advacancies are modified to values $c_1(\mathbf{r},t)$, $c_2(\mathbf{r},t)$. These depend on time t and position $\mathbf{r}$ on the terrace. The desired result is achieved by solving, for the particular case of interest here, equations that are given explicitly in an earlier publication.[22] The boundary condition[27] at fixed sinks such as step edges requires that the concentrations there take their equilibrium values: $c_i(\mathbf{r},t) = \bar{c}_i$, $i=1,2$. This choice ensures that the step edges at those locations create thermal defects at rates that correspond to thermal equilibrium. We must calculate $c_i(\mathbf{r},t)$ to find the chemical potential $\mu^*(\mathbf{r},t)$ that is consistent with the boundary conditions for the uniform defect production defined by K_1, K_2 above.

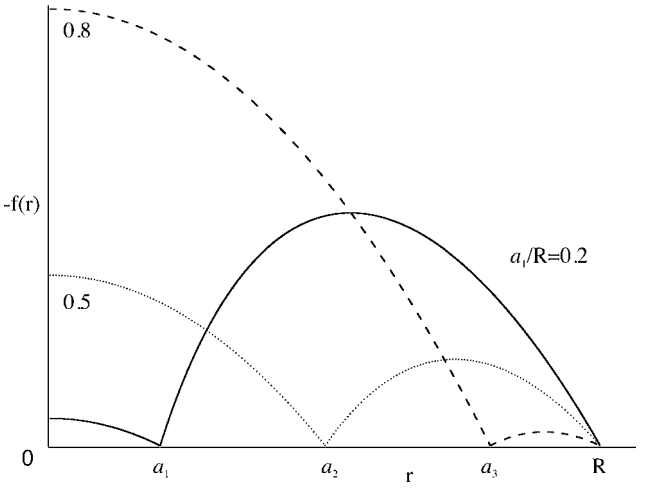

FIG. 9. Quasistatic concentration profiles [Eq.(A4)] for three different ratios of island to terrace size, a/R. The results are shown for ratios of 0.2, 0.5, and 0.8.

The theory includes reactions between antidefects, such that c_i obeys

$$\dot{c}_1 - D_1\Delta^2(c_1 - \bar{c}_1) - K_{12}(\bar{c}_1\bar{c}_2 - c_1c_2) = K_1(\mathbf{r},t),$$

$$\dot{c}_2 - D_2\nabla^2(c_2 - \bar{c}_2) - K_{12}(\bar{c}_1\bar{c}_2 - c_1c_2) = K_2(\mathbf{r},t). \quad \text{(A1)}$$

Here, K_{12} is the rate constant for antidefect reaction, with $K_{12}\bar{c}_1\bar{c}_2$ the rate per lattice site at which pairs are created, and $K_{12}c_1c_2$ the annihilation rate. D_1 and D_2 are the hopping diffusion coefficients of the two species so that the first two terms of Eqs. (A1) comprise the diffusion equation for a species in the absence of reactions and driving terms.

When the nonlinear Eqs. (A1) are linearized by writing $c_1 = \bar{c}_1 + s_1$, $c_2 = \bar{c}_2 + s_2$, and solved simultaneously for the steady state with K_1, K_2, constant, the general solutions are

$$D_1 s_1 = \frac{D_1\bar{c}_1(K_2 - K_1)}{D_1\bar{c}_1 + D_2\bar{c}_2} f(\mathbf{r}) + \frac{\mathbf{A}}{\kappa^2}\left[\frac{g_\kappa(\mathbf{r})}{g_\kappa(\rho)} - 1\right],$$

$$D_2 s_2 = \frac{D_2\bar{c}_2(K_1 - K_2)}{D_1\bar{c}_1 + D_2\bar{c}_2} f(\mathbf{r}) + \frac{\mathbf{A}}{\kappa^2}\left[\frac{g_\kappa(\mathbf{r})}{g_\kappa(\rho)} - 1\right],$$

$$\kappa^2 = K_{12}(D_1\bar{c}_1 + D_2\bar{c}_2)/D_1D_2 \quad \text{(A2)}$$

in which A is a constant given elsewhere,[22] $f(\mathbf{r})$ is the solution of the Poisson equation $\nabla^2 f = 1$ that has $f(\mathbf{r}) = 0$ for $\mathbf{r} = \boldsymbol{\rho}$, with $\boldsymbol{\rho}$ the locus of $\mathbf{r}$ that corresponds to sink sites, and $(\nabla^2 - \kappa^2)g(\mathbf{r}) = 0$, with g=1 at fixed sinks. For the reader's reference, Eqs. (A1) and (A2) are labeled Eqs. (1) and (13) in Ref. 22. Owing to the form, the second terms in Eqs. (A2) makes no net contribution to the atomic flux, leaving

$$J(\mathbf{r}) = -D_1\nabla s_1 + D_2\nabla s_2 = (K_1 - K_2)\nabla f(\mathbf{r}). \quad \text{(A3)}$$

We now adapt this result to the particular geometry of interest in the experiments reported in the text. In an idealized description, a circular island of radius a is concentric

with a circular terrace surrounded by a step bunch at radius R. Therefore the constraints on the solutions $s(\mathbf{r})$ have circular symmetry and $s_i=0$ at $r=a$ and $r=R$. The required solution for $r<a$ is

$$f_<(r) = (r^2 - a^2)/4, \tag{A4a}$$

and for $a<r<R$ the solution is

$$f_>(r) = \frac{r^2 - R^2}{4} - \frac{(a^2 - R^2)\ln(r/R)}{4\ln(a/R)} \tag{A4b}$$

The second term on the left of Eq. (4b) is a solution of Laplace's equation $\nabla^2 g(r)=0$. It is then quickly verified that the functions in Eqs. (A4a) and (A4b) solve the Poisson equation and satisfy the stated boundary conditions. The form of these solutions is illustrated for three values of a/R in Fig. 9.

These results are employed in Sec. III to obtain the rate of driven island growth on Pt(111) caused by a beam of Pt^- ions.

*Corresponding author: Michal Ondrejcek; Department of Physics, University of Illinois, Urbana-Champaign, 1110 W. Green Street, Urbana, Illinois 61801, USA. ondrejce@uiuc.edu; Tel: +1 217 333 9316; Fax: +1 217 244 2278.

[1] B. Mutaftschiev, *The Atomistic Nature of Crystal Growth* (Springer, Berlin, 2001).
[2] J. W. Evans, P. A. Thiel, and M. C. Bartelt, Surf. Sci. Rep. **61**, 1 (2006).
[3] J. W. Mullin, *Crystallization* (Butterworths, Oxford, 2001).
[4] M. Nastasi, J. K. Hirvonen, and J. W. Mayer, *Ion-Solid Interactions* (Cambridge University Press, Cambridge, England, 1996).
[5] H. Gnaser, *Low-Energy Ion Irradiation of Solid Surfaces* (Springer, Berlin, 1999).
[6] M. W. Thompson, *Defects and Radiation Damage in Metals* (Cambridge University Press, London, 1969).
[7] H.-C. Jeong and E. D. Williams, Surf. Sci. Rep. **34**, 171 (1999).
[8] E. G. Bauer, B. W. Dodson, D. J. Ehrlich, L. C. Feldman, C. P. Flynn, M. W. Geis, J. P. Harbison, R. J. Matyi, P. S. Peercy, P. M. Petroff, J. M. Phillips, G. B. Stringfellow, and A. Zangwill, J. Mater. Res. **5**, 852 (1990).
[9] T. Michely and J. Krug, *Islands, Mounds and Atoms* (Springer, Berlin, 2004).
[10] E. Chason, S. T. Picraux, J. M. Poate, J. O. Borland, M. I. Current, T. D. de la Rubia, D. J. Eaglesham, O. W. Holland, M. E. Law, C. W. Magee, J. W. Mayer, J. Melngailis, and A. F. Tasch, J. Appl. Phys. **81**, 6513 (1997).
[11] U. Valbusa, C. Boragno, and F. B. de Mongeot, J. Phys.: Condens. Matter **14**, 8153 (2002).
[12] J. E. McDonald, Am. J. Phys. **30**, 870 (1962).
[13] A. Pimpinelli and F. Villain, Physica A **204**, 521 (1994).
[14] J. J. Metois and D. E. Wolf, Surf. Sci. **298**, 71 (1993).
[15] Y. Homma, H. Hibino, T. Ogino, and N. Aizawa, Phys. Rev. B **55**, R10237 (1997).
[16] S. J. Tang, S. Kodambaka, W. Swiech, I. Petrov, C. P. Flynn, and T.-C. Chiang, Phys. Rev. Lett. **96**, 126106 (2006).
[17] M. Rajappan, W. Swiech, M. Ondrejcek, and C. P. Flynn, Philos. Mag. **87**, 4501 (2007).
[18] F. C. Frank, Discuss. Faraday Soc. **48**, 67 (1949).
[19] W. K. Burton, N. Cabrera, and F. C. Frank, Philos. Trans. R. Soc. London, Ser. A **243**, 299 (1951).
[20] R. M. Tromp and M. C. Reuter, Ultramicroscopy **36**, 99 (1991).
[21] W. Swiech, M. Rajappan, M. Ondrejcek, E. Sammann, S. Burdin, I. Petrov, and C. P. Flynn, Ultramicroscopy **108**, 646 (2008).
[22] C. P. Flynn, Phys. Rev. B **75**, 134106 (2007).
[23] C. P. Flynn, W. Swiech, M. Ondrejcek, and M. Rajappan, Phys. Rev. B **77**, 045406 (2008).
[24] C. P. Flynn, M. Ondrejcek, and W. Swiech, J. Phys.: Condens. Matter (to be published); for earlier work with pans on Si see S. Tanaka, C. C. Umbach, J. M. Blakely, R. M. Tromp, and M. Mankos, Appl. Phys. Lett. **69**, 1235 (1996).
[25] M. Ondrejcek, W. Swiech, M. Rajappan, and C. P. Flynn, Phys. Rev. B **72**, 085422 (2005).
[26] M. Rajappan, W. Swiech, M. Ondrejcek, and C. P. Flynn, J. Phys.: Condens. Matter **19**, 226006 (2007).
[27] C. P. Flynn, Phys. Rev. B **71**, 085422 (2005).
[28] R. S. Averback and T. D. de la Rubia, *Solid State Physics* (Academic, New York, 1998), Vol. 51, pp. 281–402.